Mutant forms of EGFR promote HER2 trafficking through efficient formation of HER2-EGFR heterodimers

堤, 央乃

Lung Cancer 175 (2023) 101–111

Contents lists available at ScienceDirect

Lung Cancer

journal homepage: www.elsevier.com/locate/lungcan

Mutant forms of EGFR promote HER2 trafficking through efficient formation of HER2-EGFR heterodimers

Hirono Tsutsumi [a], Eiji Iwama [a,*], Ritsu Ibusuki [a], Atsushi Shimauchi [a], Keiichi Ota [a], Yasuto Yoneshima [a], Hiroyuki Inoue [a,b], Kentaro Tanaka [a], Yoichi Nakanishi [a], Isamu Okamoto [a]

[a] Department of Respiratory Medicine, Graduate School of Medical Sciences, Kyushu University, Fukuoka, Japan
[b] Department of Respiratory Medicine, Fukuoka University School of Medicine, Fukuoka, Japan

ARTICLE INFO

Keywords:
ErbB receptors
Dimerization
Endocytosis
Lysosomes
Lung neoplasms

ABSTRACT

Introduction: Human epidermal growth factor receptor 2 (HER2) forms homodimers and is retained at the surface of cancer cells positive for *HER2* amplification. The dimerization, internalization, and intracellular trafficking of HER2 in cancer cells without *HER2* amplification have remained uncharacterized, however.
Materials and methods: HER2 homodimers and heterodimers were detected in various cell lines with the use of an in situ proximity ligation assay. The effects of wild-type or mutant forms of epidermal growth factor receptor (EGFR) on intracellular trafficking of HER2 were examined by live-cell imaging. The sensitivity of cell lines without *HER2* amplification to ado-trastuzumab emtansine (T-DM1), an anti-HER2 (trastuzumab)–cytotoxic drug conjugate (ADC) was also investigated.
Results: HER2 preferentially formed heterodimers with EGFR rather than homodimers and was rapidly internalized together with EGFR in cells without *HER2* amplification. HER2-EGFR heterodimers were more abundant and HER2 was more efficiently transferred to lysosomes in such cells with than in those without *EGFR* activating mutations. T-DM1 showed a high cytotoxic efficacy in the cells with *EGFR* mutations, suggesting that mutant forms of EGFR promote the transfer of HER2-bound T-DM1 to lysosomes through efficient formation of HER2-EGFR heterodimers.
Conclusion: Our findings reveal that HER2 trafficking is affected by EGFR, especially by mutant forms of the receptor, and they provide a rationale for the use of HER2-targeting ADCs in the treatment of *EGFR*-mutated lung cancer.

1. Introduction

The human epidermal growth factor receptor (HER) family of receptor tyrosine kinases includes the epidermal growth factor receptor (EGFR, also known as HER1 or ErbB1), HER2 (ErbB2 or Neu), HER3 (ErbB3), and HER4 (ErbB4), each of which forms homodimers or heterodimers with other family members [1,2]. Such dimerization results in receptor autophosphorylation by the intracellular tyrosine kinase domain of EGFR, HER2, or HER4 and activation of downstream signaling including that mediated by phosphatidylinositol 3-kinase (PI3K)–Akt and Ras-Raf-MEK-ERK pathways, with such signaling contributing to the regulation of cell motility, invasion, and progression in various types of cancer [3–5].

Although no natural ligand has been identified for HER2, the protein exists in a constitutively extended conformation and is thus a preferred partner for heterodimer formation by other HER family receptors [6]. On the other hand, although HER2 forms homodimers in cells with *HER2* amplification, such homodimerization appears to be infrequent in cells without *HER2* amplification because the extracellular domain of HER2 is highly negatively charged and interferes with homodimer

Abbreviations: ADC, antibody–cytotoxic drug conjugate; ANOVA, analysis of variance; Cmab-647, HiLyte Fluor 647–conjugated cetuximab; DAPI, 4′,6-diamidino-2-phenylindole; del19, deletion in exon 19; EGFR, epidermal growth factor receptor; FITC, fluorescein isothiocyanate; HER, human epidermal growth factor receptor; MFI, mean fluorescence intensity; NSCLC, non–small cell lung cancer; PBS, phosphate-buffered saline; PLA, proximity ligation assay; T-DM1, ado-trastuzumab emtansine; TKI, tyrosine kinase inhibitor; Tz-555, HiLyte Fluor 555–conjugated trastuzumab; WT, wild type.

* Corresponding author at: Department of Respiratory Medicine, Graduate School of Medical Sciences, Kyushu University, 3-1-1 Maidashi, Higashi-ku, Fukuoka 812-8582, Japan.
E-mail address: iwama.eiji.800@m.kyushu-u.ac.jp (E. Iwama).

https://doi.org/10.1016/j.lungcan.2022.11.018
Received 1 September 2022; Received in revised form 21 November 2022; Accepted 24 November 2022
Available online 29 November 2022

formation [7–9]. Most non–small cell lung cancer (NSCLC) tumors express EGFR at a high level and do not manifest *HER2* amplification, but whether EGFR is a preferred partner for heterodimer formation by HER2 in such tumor cells has remained unknown.

Dimers of HER family receptors are internalized into the cytoplasm within the endosomal compartment and are sorted either to lysosomes for degradation or to recycling endosomes for return to the cell surface. Most internalized HER2 has been shown to be recycled back to the cell membrane and to be retained at the cell surface in cells with *HER2* amplification [10–12]. The trafficking of HER2, including its internalization and transfer to lysosomes, as well as the effects of EGFR on such trafficking in cells without *HER2* amplification have not been characterized, however.

Activating mutations of *EGFR*, including in-frame deletions in exon 19 (del19) and an L858R point mutation in exon 21, are present in ~ 15 % and ~ 40 % of individuals with NSCLC in the United States and Europe and in Asia, respectively [13]. These mutations are oncogenic drivers because they induce autophosphorylation of EGFR and constitutive activation of downstream signaling [14–17]. Although such mutations promote ligand-independent homodimerization of EGFR [17,18], it has remained unclear whether they also facilitate the formation of heterodimers with HER2 or affect the internalization and intracellular trafficking of HER2.

We here applied an in situ proximity ligation assay (PLA) to detect HER2 homodimers and heterodimers in various cell lines. We also examined the effects of wild-type (WT) or mutant forms of EGFR on intracellular trafficking of HER2 with the use of live-cell imaging. Furthermore, we evaluated the sensitivity of cell lines without *HER2* amplification to ado-trastuzumab emtansine (T-DM1), an antibody–cytotoxic drug conjugate (ADC) that targets HER2.

2. Materials and methods

2.1. Cell lines and reagents

Six NSCLC cell lines with *EGFR* activating mutations (PC-9 [ECACC #90071810], II-18 [RIKEN BioResource Research Center, Tsukuba, Japan; #RCB2093], HCC4006 [ATCC #CRL-2871], HCC827 [ATCC #CRL-2868], H1975 [ATCC #CRL-5908], and H1650 [ATCC #CRL-5883]), four NSCLC cell lines WT for *EGFR* (Calu-3 [ATCC #HTB-55], A549 [ATCC #CCL-185], H1299 [ATCC #CRL-5803], and H1437 [ATCC #CRL-5872]), and five breast cancer cell lines WT for *EGFR* (BT-474 [ATCC #HTB-20], HCC1954 [ATCC #CRL-2338], T-47D [ATCC #HTB-133], MDA-MB-436 [ATCC #HTB-130], and MCF7 [ECACC #86012803]) were used in the present study. Details for each cell line including *HER2* amplification and *EGFR* mutation status are provided in Table S1. PC-9, II-18, HCC4006, HCC827, H1975, H1650, H1299, H1437, BT-474, HCC1954, and T-47D cells were cultured in RPMI 1640 (Gibco, Carlsbad, CA, USA); A549, MDA-MB-436, and MCF7 cells in Dulbecco's modified Eagle's medium (Gibco); and Calu-3 cells in Eagle's minimum essential medium (Nacalai Tesque, Kyoto, Japan). Each medium was supplemented with 10 % fetal bovine serum and 1 % penicillin–streptomycin (Gibco). All cells were maintained under a humidified atmosphere of 5 % CO_2 at 37 °C. Chloroquine (Tokyo Chemical Industry, Tokyo, Japan) and osimertinib (ChemScene, Monmouth Junction, NJ, USA) were dissolved in water or dimethyl sulfoxide (Fujifilm Wako Pure Chemical Industries, Osaka, Japan) and stored at –80 °C or –20 °C, respectively. Trastuzumab (Chugai Pharmaceutical, Tokyo, Japan), cetuximab (Merck Biopharma, Tokyo, Japan), and T-DM1 (Chugai Pharmaceutical) were stored at 4 °C. For the in situ PLA and immunofluorescence analysis, cells were grown to 70 % confluence on 12-mm-diameter coverslips (Matsunami, Osaka, Japan) placed in 24-well plates (Corning, Corning, NY, USA).

2.2. Establishment of osimertinib-resistant cell lines

Osimertinib-resistant cell lines were established by two different methods. Parental cells were thus cultured with stepwise increases in the concentration of osimertinib from 10 nM to 2 μM (PC-9_OR1 cells and HCC827_OR cells), with the medium being changed every 3 days, and the osimertinib-treated cells were maintained for 3 months. Alternatively, parental cells were exposed to *N*-nitroso-*N*-ethylurea (Sigma-Aldrich, St. Louis, MO, USA) at 50 μg/ml for 24 h and then cultured with stepwise escalation of osimertinib concentration from 200 nM to 1 μM (PC-9_OR2 cells).

2.3. Retrovirus transduction for generation of stable cell lines

For establishment of MCF7 cells stably expressing WT or mutant forms of EGFR, pBABE vectors for the WT protein (#11011; Addgene, Cambridge, MA, USA) or for del19 (#32062, Addgene) or L858R (#11012, Addgene) mutants were first introduced into HEK293T cells (ATCC #CRL-1573) with the use of a Retrovirus Packaging Kit Ampho (Takara Bio, Shiga, Japan) and the Lipofectamine 3000 reagent (Invitrogen, Carlsbad, CA, USA). Culture supernatants were passed through a 0.45-μm filter, and the filtrate was incubated overnight at 4 °C with retro-X Concentrator (Clontech, Shiga, Japan) and then centrifuged at 1500 × *g* for 45 min at 4 °C for isolation of retrovirus pellets. MCF7 cells were infected with the retroviruses for 24 h in the presence of polybrene (Nacalai Tesque) at 8 μg/ml and were then cultured in growth medium for an additional 24 h before selection by culture in the presence of puromycin (Invitrogen) at 1 μg/ml.

2.4. Flow cytometric analysis

Cells were incubated for 30 min at 4 °C with a 1:200 dilution of either fluorescein isothiocyanate (FITC)–conjugated antibodies to HER2 (#324404; BioLegend, San Diego, CA, USA), FITC-conjugated antibodies to HER3 (#10201-MM03-F; Sino Biological, Kanagawa, Japan), or FITC-conjugated isotype control antibodies (BioLegend #400109) for flow cytometric analysis with a FACSVerse instrument (BD Biosciences, Franklin Lakes, NJ, USA) in order to evaluate the expression level of HER2 at the cell surface. Cell lines other than HCC827 were incubated with a 1:200 dilution and HCC827 cells with a 1:2000 dilution of either allophycocyanin-conjugated antibodies to EGFR (BioLegend #352906) or allophycocyanin-conjugated isotype control antibodies (BioLegend #400121) to evaluate the expression level of EGFR at the cell surface. The relative mean fluorescence intensity (MFI) ratio of HER2, HER3, or EGFR was determined as the corresponding MFI divided by that of the isotype control.

2.5. Immunoblot analysis

Cultured cells were lysed in RIPA buffer (Thermo Fisher Scientific, Waltham, MA, USA), the lysates were fractionated by SDS–polyacrylamide gel electrophoresis, and the separated proteins were transferred to a polyvinylidene difluoride membrane. The membrane was incubated overnight at 4 °C with primary antibodies to phosphorylated EGFR (#3777, diluted 1:1000; Cell Signaling Technology, Danvers, MA, USA), to EGFR (#4267, diluted 1:1000; Cell Signaling Technology), to HER2 (#ab134182, diluted 1:1000; Abcam, Cambridge, MA, USA), to HER3 (#sc-81455, diluted 1:200; Santa Cruz Biotechnology, Dallas, TX, USA), and to β-actin (#4970, diluted 1:1000; Cell Signaling Technology). Immune complexes were detected with horseradish peroxidase–conjugated goat antibodies to rabbit (#NA9340V, diluted 1:10,000; GE Healthcare UK, Amersham, UK) or mouse (#NA931VS, diluted 1:10,000; GE Healthcare UK) immunoglobulin G, Pierce Western Blotting Substrate Plus (Thermo Fisher Scientific), and the ChemiDoc XRS + system (Bio-Rad, Hercules, CA, USA).

2.6. Microscopy analysis

All images were obtained with an all-in-one fluorescence microscope (BZ-X800; Keyence, Osaka, Japan) equipped with a Plan Apochromat 100 × objective (numerical aperture of 1.45; BZ-PA100, Keyence). Optical sectioning was applied to capture cross-sectional images of specimens at the focused depth so as to avoid blurred, out-of-focus images [19,20]. Optical sectioning images of cells were obtained from *z*-stacking acquired from top to bottom of each cell at 0.6-μm intervals with the use of a sectioning module (BZ-H3XF, Keyence). Images for *z*-projection were obtained with the use of a Multi Stack Module (BZ-H4XD, Keyence).

2.7. In situ PLA

The in situ PLA technique, which can detect interaction of protein molecules in close proximity [18,21], was adopted to identify HER2 homodimers or heterodimers. In brief, cells were fixed for 15 min with 4 % paraformaldehyde in phosphate-buffered saline (PBS), permeabilized for 10 min with 0.3 % Triton X-100 in PBS, and incubated overnight at 4 °C with 1:500 dilutions of rabbit antibodies to HER2 (Abcam #ab134182) and mouse antibodies to HER2 (Thermo Fisher Scientific #MA5-13675) for detection of HER2 homodimers; the mouse antibodies to HER2 and rabbit antibodies to EGFR (Abcam #ab32077) for detection of HER2-EGFR heterodimers; and the rabbit antibodies to HER2 and mouse antibodies to HER3 (Santa Cruz Biotechnology #sc-81455) for detection of HER2-HER3 heterodimers. HER2 homodimers and HER2 heterodimers with EGFR or HER3 were detected with the use of Duolink PLA Fluorescence Kits (Sigma-Aldrich #DUO92002, −92004, and 92014, respectively). Images of PLA signals were obtained with the BZ-X800 all-in-one fluorescence microscope (Keyence). The number of PLA signals was quantified in 50 cells for each cell line with the use of BZ-X Analyzer software (BZ-H4A, Keyence). Optical sectioning images of HER2-EGFR heterodimers in multiple cells acquired from top to bottom of each cell were combined into a *z*-projection image with the use of full-focus imaging (BZ-H4A, Keyence).

2.8. Preparation of fluorescently labeled trastuzumab and cetuximab

Trastuzumab and cetuximab were fluorescently labeled with the use of a HiLyte Fluor 555 Labeling Kit-NH2 (LK14; Dojindo, Kumamoto, Japan) and HiLyte Fluor 647 Labeling Kit-NH2 (LK15, Dojindo), yielding HiLyte Fluor 555–conjugated trastuzumab (Tz-555) and HiLyte Fluor 647–conjugated cetuximab (Cmab-647), respectively. The kits label amino acid residues of the antibodies with 3 to 7 dye molecules per antibody molecule. Tz-555 and Cmab-647 were applied for analysis of the trafficking of HER2 and EGFR, respectively.

2.9. Live-cell imaging

Cells were transferred to μ-Slide eight-well plates (Ibidi, Gräfelfing, Germany) at a density of 2×10^4 cells per well in a volume of 300 μl. After culture for 24 h, the cells were incubated for 30 min at 4 °C with a 1:500 dilution of Tz-555 with or without a 1:500 dilution of Cmab-647. They were then washed three times with ice-cold PBS to remove unbound Tz-555 or Cmab-647 before the addition of warmed culture medium and incubation at 37 °C under 5 % CO_2 in the stage-top chamber of the BZ-X800 all-in-one fluorescence microscope (Keyence). Images were captured every 10 min and edited to generate a time-lapse movie and to quantify the percentage area of internalized Tz-555 signals with the use of BZ-X Analyzer software (BZ-H4A, Keyence).

2.10. Immunofluorescence analysis for evaluation of colocalization of HER2 with either early endosomes or lysosomes

For the detection of colocalization of HER2 and early endosomes, cells were incubated for 30 min at 4 °C with a 1:500 dilution of Tz-555, washed three times with ice-cold PBS to remove unbound Tz-555, and then incubated for 30 min at 37 °C under 5 % CO_2. The cells were fixed for 15 min with 4 % paraformaldehyde, permeabilized for 10 min with 0.3 % Triton X-100, exposed to Block Ace (KAC, Kyoto, Japan) for 1 h at room temperature, and then incubated first overnight at 4 °C with a 1:100 dilution of antibodies to EEA1 (#3288, Cell Signaling Technology) in 10 % Block Ace and then for 1 h at room temperature with a 1:500 dilution of Alexa Fluor 488–conjugated goat antibodies to rabbit immunoglobulin G (GE Healthcare UK) in 10 % Block Ace. For the detection of colocalization of HER2 and lysosomes, cells were exposed to medium containing chloroquine (50 μM) for 24 h, incubated for 30 min at 4 °C with a 1:500 dilution of Tz-555, washed three times with ice-cold PBS to remove unbound Tz-555, and then incubated for 2 h at 37 °C under 5 % CO_2 in medium containing chloroquine (50 μM). The cells were fixed for 15 min with 4 % paraformaldehyde and permeabilized for 10 min with 0.3 % Triton X-100 before exposure to Block Ace for 1 h at room temperature and incubation overnight at 4 °C with a 1:1000 dilution of Alexa Fluor 488–conjugated antibodies to LAMP1 (#328610, BioLegend) in 10 % Block Ace. Images were obtained with the BZ-X800 all-in-one fluorescence microscope (Keyence), and the area of fluorescence signals was quantified in nine images for each cell line with the use of BZ-X Analyzer software (BZ-H4A, Keyence) to determine the percentage of trastuzumab colocalizing with LAMP1.

2.11. Cell viability assay

Cells were plated in 96-well plates (5×10^3 cells/well) and cultured for 24 h before the addition of T-DM1 or osimertinib at various concentrations and incubation for an additional 72 h. Cell viability was then determined with the use of a Cell Counting Kit-8 (Dojindo).

2.12. Statistical analysis

Data were compared with the unpaired Student's *t* test, one-way analysis of variance (ANOVA), the Mann-Whitney test, or Spearman correlation analysis as performed with GraphPad Prism 8 software. A p value of < 0.05 was considered statistically significant.

3. Results

3.1. HER2 preferentially forms heterodimers with EGFR in cell lines without HER2 amplification

The expression level of HER2 as detected by flow cytometry and immunoblot analysis was much higher in cancer cell lines with *HER2* amplification than in those without such amplification, regardless of *EGFR* activating mutation status or cancer type (lung cancer or breast cancer) (Fig. S1A, C). To examine the dimerization partners of HER2 in such cells, we applied a PLA to detect HER2 homodimers or heterodimers with EGFR or HER3. Optical sectioning of cells showed that HER2 homodimers are abundant in cell lines with *HER2* amplification, with such homodimers being detected mostly at the cell surface in these cell lines (Fig. 1A). In cell lines without *HER2* amplification, however, HER2 homodimers were rarely detected, irrespective of the expression level of HER2 (Fig. 1B, C), consistent with the previous finding that HER2 homodimerization is infrequent in cells negative for *HER2* amplification [7–9]. In the cell lines without *HER2* amplification, EGFR was the predominant dimerization partner of HER2, with HER2-EGFR heterodimers being detected in the cytoplasm (Fig. 1B, C). These findings suggested that HER2 dimerizes preferentially with EGFR and localizes to the cytoplasm together with EGFR in lung and breast cancer cell lines without *HER2* amplification.

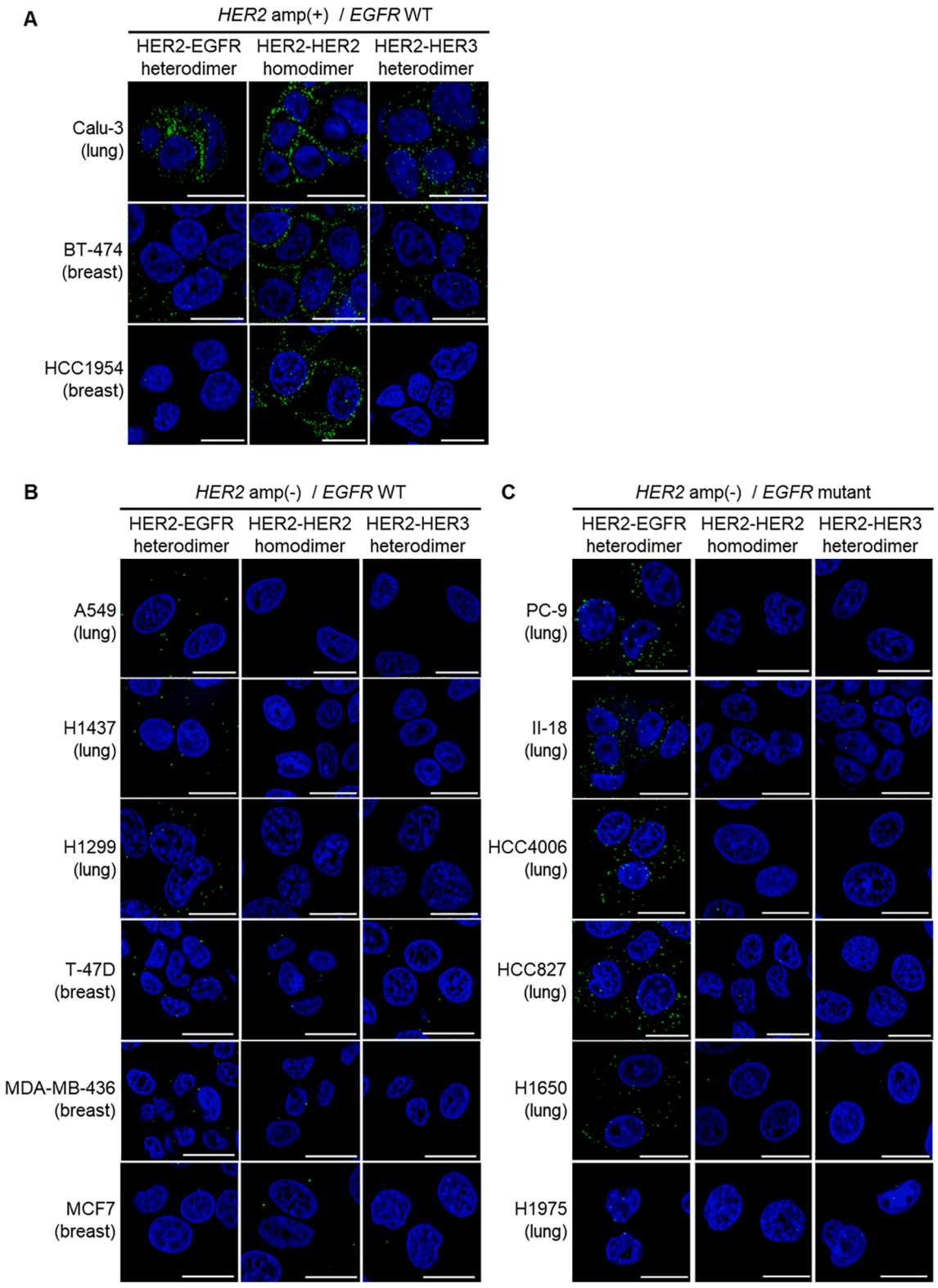

Fig. 1. Detection of HER2 homodimers and heterodimers with an in situ PLA in cancer cell lines. Lung or breast cancer cell lines positive for *HER2* amplification (amp) and WT for *EGFR* (**A**) as well as those without *HER2* amplification and either negative (**B**) or positive (**C**) for *EGFR* activating mutations were subjected to a PLA (green signals) for detection of HER2 homodimers or HER2-EGFR or HER2-HER3 heterodimers. The representative images were obtained by optical sectioning. Nuclei (blue signals) were stained with 4′,6-diamidino-2-phenylindole (DAPI). Scale bars, 20 μm.

3.2. HER2-EGFR heterodimers are more abundant in cell lines with than in those without EGFR activating mutations

To evaluate all PLA signals for HER2-EGFR heterodimers in cell lines without *HER2* amplification, we constructed digital images in which multiple optical sectioning images are combined in a *z*-projection (Fig. 2A, B). Quantification of the PLA signals showed that the number of HER2-EGFR heterodimers per cell was significantly higher for cell lines

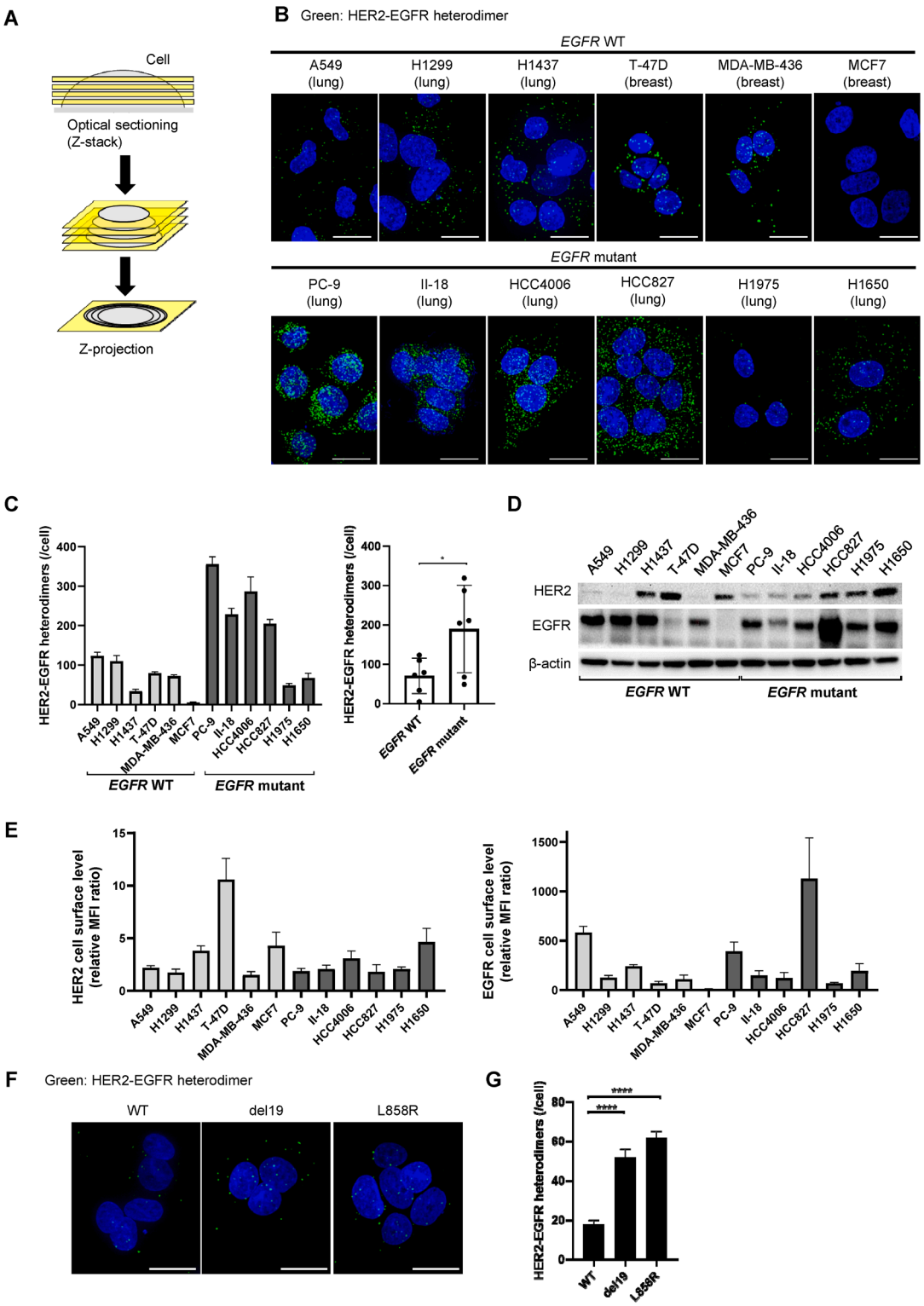

Fig. 2. *EGFR* activating mutations promote HER2-EGFR heterodimerization in cancer cell lines without *HER2* amplification. (**A**) *z*-Projection images were constructed by combination of optical sectioning images of multiple cells obtained by *z*-stacking. (**B**) Representative *z*-projection images obtained with an in situ PLA for HER2-EGFR heterodimers (green signals) in lung or breast cancer cell lines negative for *HER2* amplification and either negative or positive for *EGFR* activating mutations. Nuclei (blue signals) were stained with DAPI. Scale bars, 20 μm. (**C**) Quantification of the number of HER2-EGFR heterodimers per cell from images as in (**B**). Data are means + SEM (left, $n = 50$ cells) or means ± SD (right, $n = 6$ cell lines). *$p < 0.05$ (unpaired Student's *t* test). (**D**) Immunoblot analysis of HER2 and EGFR in lung and breast cancer cell lines. β-actin was examined as a loading control. (**E**) Relative MFI ratios for expression of HER2 and EGFR at the cell surface determined by flow cytometric analysis. Data are means + SD from three independent experiments. (**F**) Representative *z*-projection images obtained with an in situ PLA performed as in (**B**) for HER2-EGFR heterodimers in MCF7 cells infected with retroviruses encoding WT or mutant (del19 or L858R) forms of EGFR. (**G**) Number of HER2-EGFR heterodimers per cell for cells as in (**F**). Data are means + SEM ($n = 50$ cells). ****$p < 0.0001$ (one-way ANOVA). All data are representative of or from three independent experiments.

with *EGFR* activating mutations than for those WT for *EGFR* (Fig. 2C). The number of HER2-EGFR heterodimers did not appear to be affected by the expression level of EGFR or HER2 as assessed by immunoblot analysis or flow cytometry (Fig. 2D, E; Figs. S1 and S2). The number of HER2-EGFR heterodimers per cell was also significantly higher in MCF7 cells infected with retroviruses encoding mutant (del19 or L858R) forms of EGFR than in those infected with a virus encoding the WT protein (Fig. 2F, G; Fig. S3). These results indicated that *EGFR* activating mutations promote the formation of HER2-EGFR heterodimers in cancer cells without *HER2* amplification.

3.3. HER2 is rapidly internalized in cells negative for HER2 amplification regardless of EGFR activating mutation status

To investigate whether *EGFR* activating mutations affect the internalization of HER2, we monitored HER2 by live-cell imaging in cell lines with or without such mutations. HER2 at the cell surface was labeled with Tz-555 (HiLyte Fluor 555–conjugated trastuzumab) at 4 °C, and receptor internalization was then induced by incubation of the cells at 37 °C. Live-cell imaging showed that HER2 internalization began within 30 min and increased with time in NSCLC cell lines without *HER2* amplification regardless of *EGFR* activating mutation status (Fig. 3A, Fig. S4A, and Movie S1A–D). By contrast, in Calu-3 and BT-474 cells, which are positive for *HER2* amplification, most HER2 remained at the cell surface for at least 60 min, with intracellular HER2 being finally apparent after 4 h (Fig. 3B, Fig. S4B, and Movie S1E, F), consistent with previous findings [13]. Rapid internalization of HER2 was also observed in MCF7 cells infected with retroviruses encoding WT or mutant (del19 or L858R) forms of EGFR (Fig. 3C, Fig. S4C, and Movie S1G–I). These results suggested that HER2 is rapidly internalized in cell lines without *HER2* amplification regardless of *EGFR* activating mutation status compared with those with *HER2* amplification.

3.4. HER2 is internalized together with EGFR in HER2 amplification–negative cells

On the basis of our findings that HER2 preferentially forms heterodimers with EGFR in cells negative for *HER2* amplification and is rapidly internalized in such cells, we investigated whether HER2 internalization might occur concomitantly with that of EGFR. PC-9 and A549 were examined as representative cell lines that express mutant or WT forms of EGFR, respectively, and in which the expression levels of HER2 and EGFR are each similar (Fig. 2D, Fig. S1). Cells were exposed to Tz-555 and to Cmab-647 (HiLyte Fluor 647–conjugated cetuximab) at 4 °C in order to monitor trafficking of HER2 and EGFR, respectively, by live-cell imaging. In both PC-9 and A549 cells, internalization of Cmab-647, like that of Tz-555, was observed at 30 min after the onset of incubation at 37 °C. Of note, almost all Tz-555 signals colocalized with Cmab-647 signals during the internalization of EGFR (Fig. 4, Movie S2). These findings suggested that the rapid internalization of HER2 in cell lines without *HER2* amplification is associated with the dimerization of HER2 with EGFR.

3.5. HER2 is more efficiently transferred to lysosomes in cell lines with EGFR activating mutations

To investigate the trafficking of HER2 to early endosomes or lysosomes, we performed immunofluorescence analysis with antibodies to the early endosome marker EEA1 and to the lysosome marker LAMP1, respectively. Tz-555 colocalized with EEA1 in both A549 and PC-9 cells at 30 min, suggesting that HER2 is initially present in early endosomes after the onset of internalization (Fig. S5). Cells were also exposed to chloroquine to inhibit the degradation of HER2 and EGFR by lysosomes and were allowed to internalize Tz-555 for 2 h at 37 °C. We then quantified the colocalization of Tz-555 signals with LAMP1 signals in PC-9 and A549 cells. The extent of Tz-555 colocalization with LAMP1 was significantly greater in PC-9 cells than in A549 cells, with the former cells also showing enlarged LAMP1-positive structures (Fig. 5A, B). In both cell lines, HER2 was found to retain its association with EGFR even after 2 h of incubation at 37 °C (Fig. S6), suggesting that HER2 was transferred to lysosomes as a heterodimer with EGFR. MCF7 cells forcibly expressing mutant (del19 or L858R) forms of EGFR also manifested more enlarged LAMP1-positive structures and a significantly greater extent of Tz-555 colocalization with LAMP1 compared with those stably expressing the WT protein (Fig. 5C, D). These findings indicated that activating mutations of *EGFR* promote the transfer of HER2 to lysosomes.

3.6. EGFR activating mutation–positive cells are sensitive to T-DM1

We found that HER2 formed more HER2-EGFR heterodimers and was more efficiently transferred to lysosomes in cells with *EGFR* activating mutations compared with those without such mutations. Given that T-DM1 selectively binds to HER2 at the cell surface and is then internalized into the cytoplasm and transferred to lysosomes, resulting in release of the cytotoxic drug, we examined the cytotoxicity of T-DM1 in cells with *EGFR* activating mutations. Although sensitivity to T-DM1 appeared to be related to HER2 expression level at the cell surface for most cell lines without *EGFR* mutations, several *EGFR* activating mutation–positive cell lines—including PC-9, II-18, HCC4006, and HCC827—that express HER2 at a low level were as sensitive to T-DM1 as were cell lines positive for *HER2* amplification (Fig. 6A). MCF7 cells stably expressing mutant forms of EGFR were also more sensitive to T-DM1 than were those expressing the WT protein (Fig. 6B), confirming that *EGFR* activating mutations increase cell sensitivity to T-DM1.

Finally, we tested whether such high sensitivity to T-DM1 was retained in *EGFR* activating mutation–positive cells that acquire resistance to the EGFR tyrosine kinase inhibitor (TKI) osimertinib. We established two osimertinib-resistant PC-9 cell lines—PC-9_OR1 and PC-9_OR2 (Fig. S7A)—in which neither *HER2* amplification (Fig. S7B), an increase in the number of HER2-EGFR heterodimers (Fig. S7C, D), nor the C797S point mutation of *EGFR* (data not shown) was detected as a potential resistance mechanism. The two osimertinib-resistant cell lines retained high sensitivity to T-DM1, with median inhibitory concentration (IC_{50}) values of 2.6, 7.8, and 1.0 μg/ml for parental PC-9, PC-9_OR1, and PC-9_OR2 cells, respectively (Fig. S7E). Similar results were obtained with parental and osimertinib-resistant (HCC827_OR) HCC827 cells (Fig. S8). These findings thus suggested that T-DM1 is effective for cells with *EGFR* activating mutations regardless of whether these cells have acquired resistance to EGFR-TKIs or not.

4. Discussion

Amplification of *HER2* is associated with cancer progression, and various HER2-targeted drugs have been developed for several types of cancer with this genetic alteration. HER2 forms homodimers and is retained at the cell surface in cancer cells with *HER2* amplification [10–12]. However, the dimerization pattern and trafficking of HER2 in cancer cells without *HER2* amplification have remained unknown.

We have now applied an in situ PLA to investigate the dimerization pattern of HER2. Although HER2 homodimers were predominant in cancer cell lines with *HER2* amplification, HER2 preferentially formed heterodimers with EGFR in those negative for *HER2* amplification. The number of HER2-EGFR heterodimers was higher in *HER2* amplification–negative cell lines with *EGFR* activating mutations than in those WT for *EGFR*. We previously showed that EGFR homodimers are more abundant in cell lines positive for *EGFR* activating mutations than in those negative for such mutations [18]. Together, our results thus suggest that conformational changes of EGFR associated with activating mutations result in ligand-independent formation of EGFR homodimers or HER2-EGFR heterodimers.

HER2 is internalized slowly and is mostly recycled back to the cell

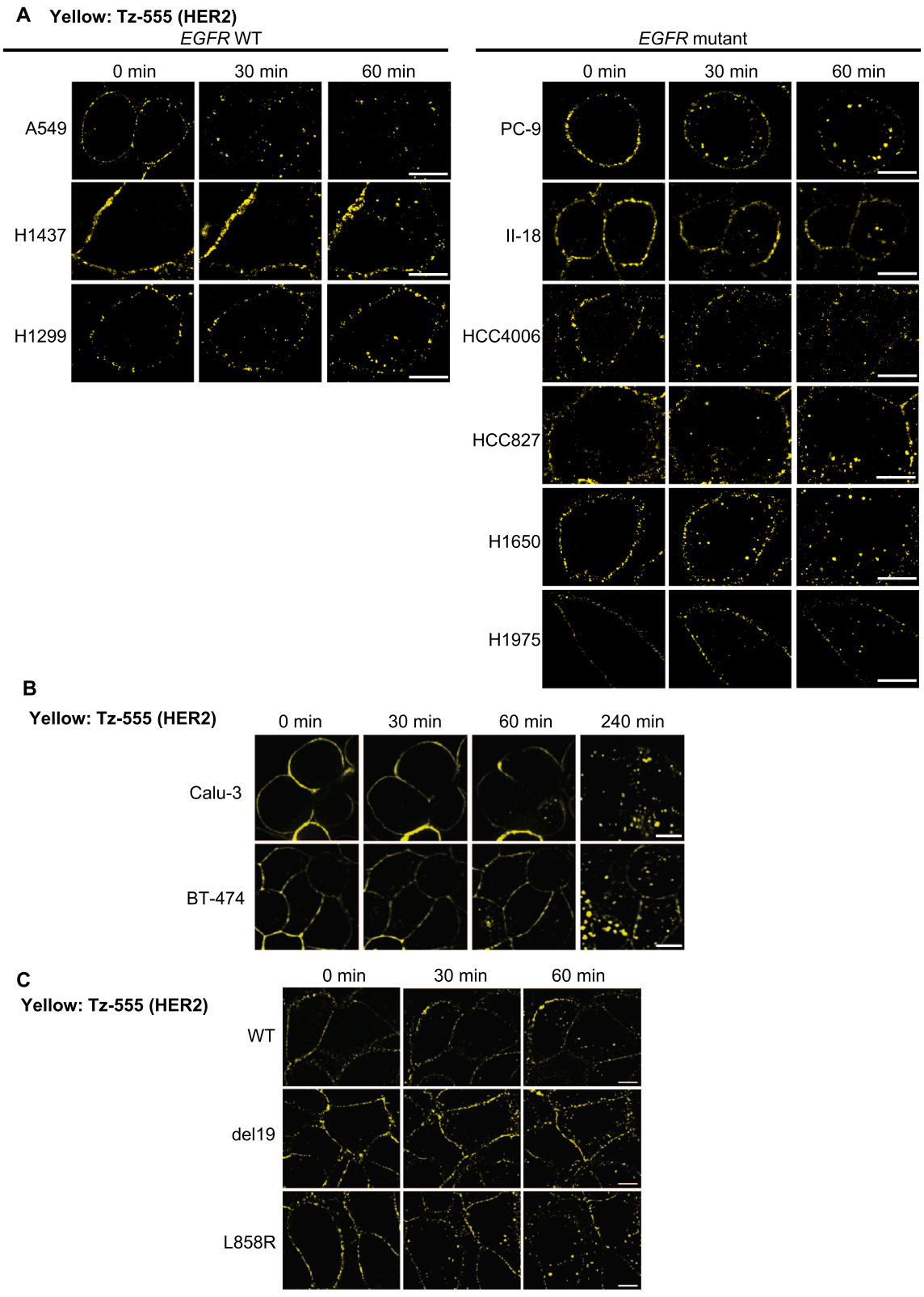

Fig. 3. HER2 is rapidly internalized in cancer cell lines negative for *HER2* amplification. *HER2* amplification–negative lung cancer cell lines (**A**), *HER2* amplification–positive cell lines (**B**), and MCF7 cells infected with retroviruses encoding WT or mutant (del19 or L858R) forms of EGFR (**C**) were exposed to Tz-555 at 4 °C for 30 min, washed, and incubated at 37 °C beginning at time 0 min for live-cell imaging of Tz-555–labeled HER2 (yellow). Data are representative of two independent experiments. Scale bars, 10 μm.

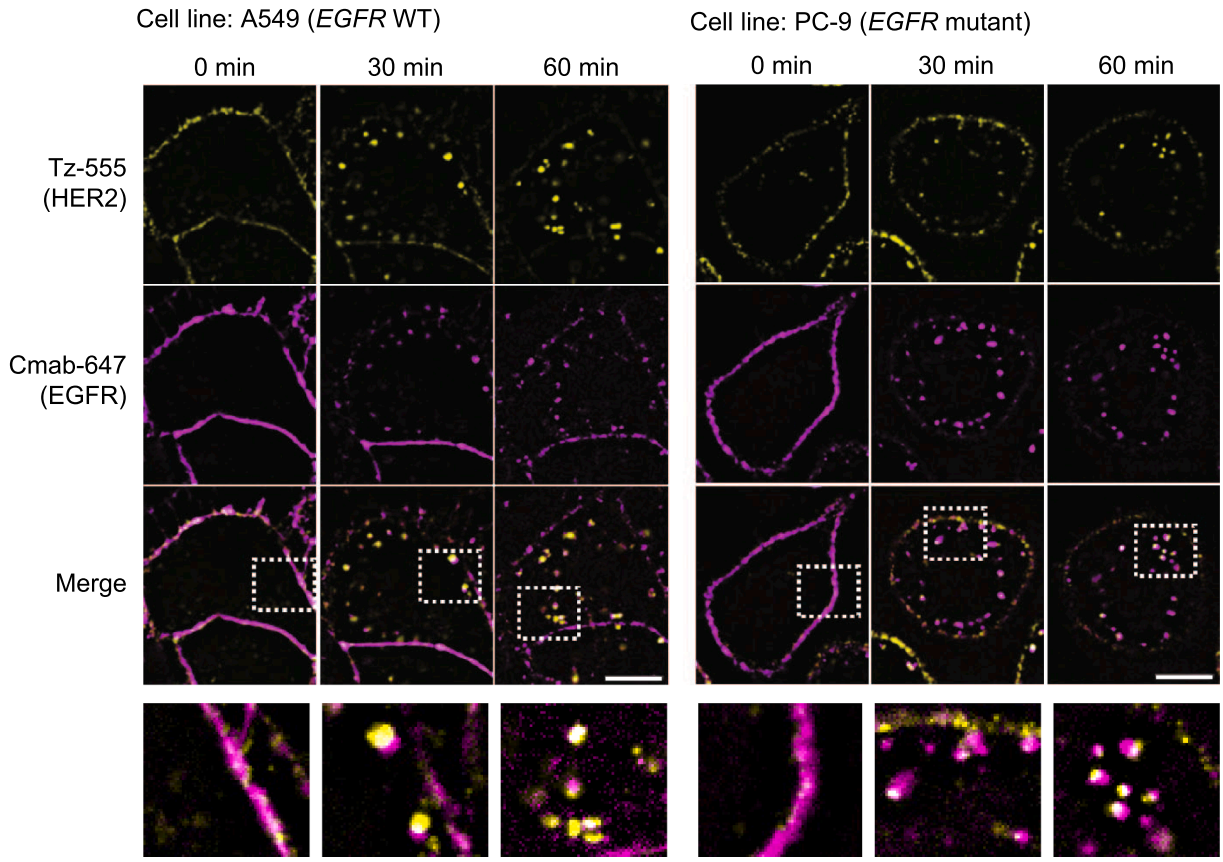

Fig. 4. HER2 is internalized together with EGFR in *HER2* amplification–negative cancer cell lines. A549 and PC-9 cells were exposed to Tz-555 and Cmab-647 at 4 °C for 30 min, washed, and incubated at 37 °C beginning at time 0 min for live-cell imaging of Tz-555–labeled HER2 (yellow) and Cmab-647–labeled EGFR (purple). Colocalization of Tz-555 and Cmab-647 signals is indicated in white in the merged images, with the boxed regions of the upper merged panels being shown at higher magnification in the lower panels. Data are representative of two independent experiments. Scale bars, 10 μm.

surface in cell lines with *HER2* amplification [10–12]. On the other hand, EGFR is internalized rapidly and mostly transferred to lysosomes for degradation [22,23]. We have now shown that most HER2 is rapidly internalized into the cytoplasm together with EGFR in lung cancer cell lines negative for *HER2* amplification. In addition, whereas most PLA signals for HER2 homodimers were located at the cell surface of cell lines with *HER2* amplification, those for HER2-EGFR heterodimers were distributed in the cytoplasm of those without such amplification. These findings suggest that the active trafficking of EGFR facilitates the internalization of HER2 in the form of HER2-EGFR heterodimers.

We found enlarged structures positive for the lysosome marker LAMP1 as well as an increased colocalization of HER2 with LAMP1 in cells positive for *EGFR* activating mutations compared with those negative for such mutations. Such enlarged LAMP1-positive structures have previously been associated with rapid transfer of HER2 from the cell surface to lysosomes [24]. Given that activation of Akt signaling has been found to be important for the transition of EGFR from early endosomes to late endosomes [25], our findings suggest that constitutive activation of Akt signaling induced by autophosphorylation of mutant EGFR might prompt the transfer of HER2 to lysosomes mediated by formation of HER2-EGFR heterodimers.

We also found that cells with *EGFR* activating mutations tend to be more sensitive to T-DM1 than do those without such mutations. Given that the internalization and lysosomal degradation of T-DM1 are essential for its efficacy [26,27], the increased ability of mutant EGFR to form HER2-EGFR heterodimers and the consequent increased internalization of such heterodimers and their efficient transfer to lysosomes likely explain the increased T-DM1 sensitivity of cell lines with *EGFR* activating mutations.

There are several limitations of the present study. First, although we evaluated the internalization of HER2 and its transfer to lysosomes with the use of the HER2-targeted antibody trastuzumab, we did not examine the dynamics of T-DM1 and their relation to HER2-EGFR heterodimers or the expression level of HER2. Second, we found that two *EGFR* mutation–positive cell lines, H1975 and H1650, were less sensitive to T-DM1 than were the other such cell lines examined (Fig. 6A). This difference might be explained by the relatively low number of HER2-EGFR heterodimers in these two cell lines compared with the other cell lines with *EGFR* activating mutations that were sensitive to T-DM1 (Fig. 2C). Alternatively, H1650 cells do not express the tumor suppressor protein PTEN (phosphatase and tensin homolog); given that the loss of PTEN has been shown to delay EGFR trafficking from late endosomes to lysosomes [28], T-DM1 might not be efficiently degraded in lysosomes of H1650 cells. These findings suggest that collaboration between Akt and PTEN in regulation of intracellular EGFR trafficking might affect the efficacy of T-DM1.

Although EGFR-TKIs have shown excellent efficacy for *EGFR* activating mutation–positive NSCLC and have improved the survival of individuals with this disease, resistance to these drugs inevitably develops [29–31]. Amplification of *HER2* or *HER3* has been implicated in the acquisition of resistance to EGFR-TKIs [32,33]. Several ADCs that target HER2 or HER3 are currently under investigation for their ability to overcome EGFR-TKI resistance [34–36]. Patritumab-deruxtecan is thus an anti-HER3 ADC whose development is based on the upregulation of HER3 associated with acquired resistance to EGFR-TKIs [34,37]. We here showed that the high sensitivity of *EGFR*-mutated cells to T-DM1 was retained even after the development of resistance to the EGFR-TKI osimertinib by a mechanism other than *HER2* amplification,

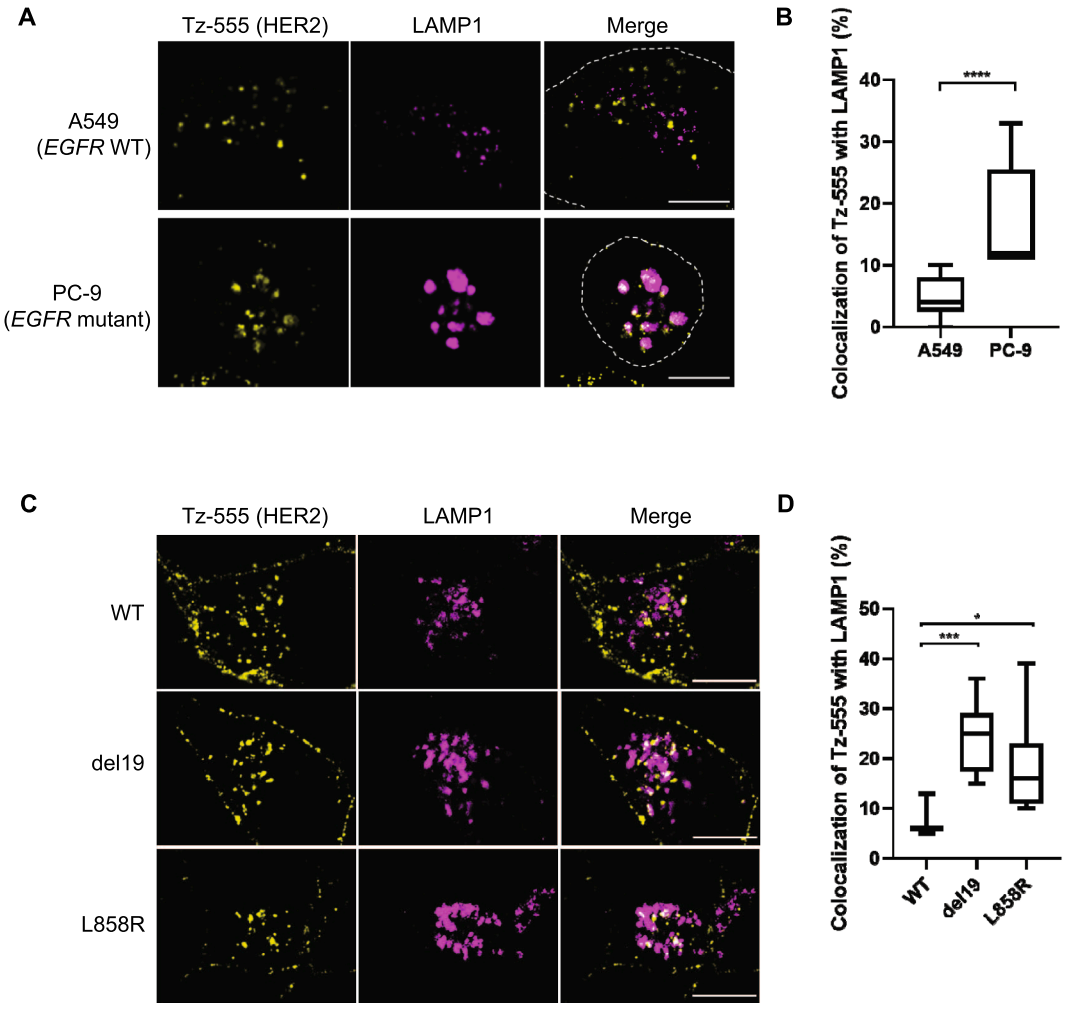

Fig. 5. Internalized HER2 is efficiently transferred to lysosomes in *EGFR* mutation–positive cancer cells. (**A**) A549 and PC-9 cells were exposed to chloroquine, labeled with Tz-555 for 30 min at 4 °C, and then incubated for 2 h at 37 °C in the presence of chloroquine, after which they were stained with antibodies to LAMP1 and both Tz-555 (yellow) and LAMP1 (purple) signals were detected by fluorescence microscopy. Colocalization of Tz-555 and LAMP1 signals is indicated in white in the merged panels. Dashed lines indicate cell boundaries. Scale bars, 10 μm. (**B**) Quantification of Tz-555 colocalization with LAMP1 in cells as in (**A**). (**C**) MCF7 cells stably expressing WT or mutant (del19 or L858R) forms of EGFR were analyzed as in (**A**). Scale bars, 10 μm. (**D**) Quantification of Tz-555 colocalization with LAMP1 in cells as in (**C**). The representative images in (**A**) and (**C**) were obtained by optical sectioning. The quantitative data ($n = 9$ fields) in (**B**) and (**D**) are presented as box plots, with the boxes representing the median and 25th and 75th percentiles and the whiskers extending to maximum and minimum values. $^{*}p < 0.05$, $^{***}p < 0.001$ (Mann-Whitney test); $^{****}p < 0.0001$ (unpaired Student's *t* test). All data are representative of three independent experiments.

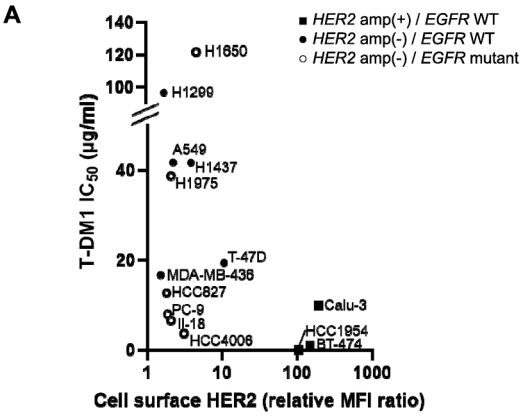

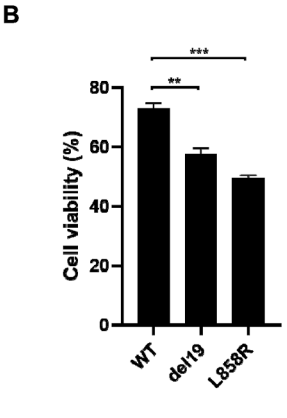

Fig. 6. *EGFR* activating mutations increase cell sensitivity to T-DM1. (**A**) Relation between the relative MFI ratio for HER2 at the cell surface and the median inhibitory concentration (IC_{50}) value for cytotoxicity of T-DM1 for cancer cell lines classified according to *HER2* amplification and *EGFR* activating mutation status. Data for MCF7 cells are not shown because the IC_{50} value was > 500 μg/ml. Data are means of triplicates from one experiment and are representative of three independent experiments. (**B**) Percentage cell viability for MCF7 cells stably expressing WT or mutant (del19 or L858R) forms of EGFR and exposed to T-DM1 (100 μg/ml) for 72 h. Data are means + SEM ($n = 3$ triplicates from one experiment, with the data being representative of three independent experiments). $^{**}p < 0.01$, $^{***}p < 0.001$ (one-way ANOVA).

suggesting that HER2-targeting ADCs have the potential to overcome osimertinib resistance even if *HER2* amplification is not responsible for the development of such resistance. Given that the efficacy of trastuzumab is not dependent on its internalization but rather on antibody-dependent cellular cytotoxicity [38], anti-HER2 ADCs are thought to have a greater cytotoxic potential than trastuzumab for

EGFR-mutated lung cancer. Our finding of increased sensitivity to T-DM1 mediated by efficient formation of HER2-EGFR heterodimers in *EGFR*-mutated cells may provide the rationale for a treatment strategy based on the administration of such ADCs to overcome resistance to EGFR-TKIs.

5. Conclusion

In conclusion, we found that HER2 preferentially forms heterodimers with EGFR rather than homodimers in cell lines without *HER2* amplification, and that such heterodimer formation occurs to a greater extent in cells with *EGFR* activating mutations. We also found that HER2 trafficking is affected by EGFR as a result of HER2-EGFR heterodimer formation in cells without *HER2* amplification, with HER2 being efficiently transferred to lysosomes in cells with *EGFR* activating mutations. These findings suggest the potential of HER2-targeting ADCs for the treatment of *EGFR*-mutated lung cancer.

Funding

This work was supported by Japan Society for the Promotion of Science [KAKENHI Grant No JP21K07100].

CRediT authorship contribution statement

Hirono Tsutsumi: Conceptualization, Methodology, Investigation, Writing – original draft, Writing – review & editing. **Eiji Iwama:** Conceptualization, Methodology, Investigation, Writing – original draft, Writing – review & editing, Funding acquisition, Supervision. **Ritsu Ibusuki:** Methodology, Investigation. **Atsushi Shimauchi:** Methodology, Investigation. **Keiichi Ota:** Writing – review & editing. **Yasuto Yoneshima:** Writing – review & editing. **Hiroyuki Inoue:** Writing – review & editing. **Kentaro Tanaka:** Writing – review & editing. **Yoichi Nakanishi:** Writing – review & editing, Supervision. **Isamu Okamoto:** Writing – review & editing, Funding acquisition, Supervision.

Declaration of Competing Interest

The authors declare that they have no known competing financial interests or personal relationships that could have appeared to influence the work reported in this paper.

Appendix A. Supplementary data

Supplementary data to this article can be found online at https://doi.org/10.1016/j.lungcan.2022.11.018.

References

[1] M.A. Olayioye, R.M. Neve, H.A. Lane, N.E. Hynes, The ErbB signaling network: receptor heterodimerization in development and cancer, EMBO J. 19 (13) (2000) 3159–3167.
[2] A.W. Burgess, H.S. Cho, C. Eigenbrot, K.M. Ferguson, T.P. Garrett, D.J. Leahy, M. A. Lemmon, M.X. Sliwkowski, C.W. Ward, S. Yokoyama, An open-and-shut case? Recent insights into the activation of EGF/ErbB receptors, Mol. Cell 12 (3) (2003) 541–552.
[3] J. Schlessinger, Ligand-induced, receptor-mediated dimerization and activation of EGF receptor, Cell 110 (6) (2002) 669–672.
[4] M.A. Lemmon, J. Schlessinger, Cell signaling by receptor tyrosine kinases, Cell 141 (7) (2010) 1117–1134.
[5] P. Seshacharyulu, M.P. Ponnusamy, D. Haridas, M. Jain, A.K. Ganti, S.K. Batra, Targeting the EGFR signaling pathway in cancer therapy, Expert Opin. Ther. Targets 16 (1) (2012) 15–31.
[6] M.M. Moasser, The oncogene HER2: its signaling and transforming functions and its role in human cancer pathogenesis, Oncogene 26 (45) (2007) 6469–6487.
[7] R. Worthylake, L.K. Opresko, H.S. Wiley, ErbB-2 amplification inhibits down-regulation and induces constitutive activation of both ErbB-2 and epidermal growth factor receptors, J. Biol. Chem. 274 (13) (1999) 8865–8874.
[8] T.P. Garrett, N.M. McKern, M. Lou, T.C. Elleman, T.E. Adams, G.O. Lovrecz, M. Kofler, R.N. Jorissen, E.C. Nice, A.W. Burgess, C.W. Ward, The crystal structure of a truncated ErbB2 ectodomain reveals an active conformation, poised to interact with other ErbB receptors, Mol. Cell 11 (2) (2003) 495–505.
[9] R. Ghosh, A. Narasanna, S.E. Wang, S. Liu, A. Chakrabarty, J.M. Balko, A. M. Gonzalez-Angulo, G.B. Mills, E. Penuel, J. Winslow, J. Sperinde, R. Dua, S. Pidaparthi, A. Mukherjee, K. Leitzel, W.J. Kostler, A. Lipton, M. Bates, C. L. Arteaga, Trastuzumab has preferential activity against breast cancers driven by HER2 homodimers, Cancer Res. 71 (5) (2011) 1871–1882.
[10] A.M. Hommelgaard, M. Lerdrup, B. van Deurs, Association with membrane protrusions makes ErbB2 an internalization-resistant receptor, Mol. Biol. Cell 15 (4) (2004) 1557–1567.
[11] C.D. Austin, A.M. De Maziere, P.I. Pisacane, S.M. van Dijk, C. Eigenbrot, M. X. Sliwkowski, J. Klumperman, R.H. Scheller, Endocytosis and sorting of ErbB2 and the site of action of cancer therapeutics trastuzumab and geldanamycin, Mol. Biol. Cell 15 (12) (2004) 5268–5282.
[12] V. Bertelsen, E. Stang, The Mysterious Ways of ErbB2/HER2 Trafficking, Membranes (Basel) 4 (3) (2014) 424–446.
[13] Y. Kobayashi, T. Mitsudomi, Not all epidermal growth factor receptor mutations in lung cancer are created equal: Perspectives for individualized treatment strategy, Cancer Sci. 107 (9) (2016) 1179–1186.
[14] T. Okabe, I. Okamoto, K. Tamura, M. Terashima, T. Yoshida, T. Satoh, M. Takada, M. Fukuoka, K. Nakagawa, Differential constitutive activation of the epidermal growth factor receptor in non-small cell lung cancer cells bearing EGFR gene mutation and amplification, Cancer Res. 67 (5) (2007) 2046–2053.
[15] H. Greulich, T.H. Chen, W. Feng, P.A. Janne, J.V. Alvarez, M. Zappaterra, S. E. Bulmer, D.A. Frank, W.C. Hahn, W.R. Sellers, M. Meyerson, Oncogenic transformation by inhibitor-sensitive and -resistant EGFR mutants, PLoS Med. 2 (11) (2005) e313.
[16] J. Cho, L. Chen, N. Sangji, T. Okabe, K. Yonesaka, J.M. Francis, R.J. Flavin, W. Johnson, J. Kwon, S. Yu, H. Greulich, B.E. Johnson, M.J. Eck, P.A. Janne, K. K. Wong, M. Meyerson, Cetuximab response of lung cancer-derived EGF receptor mutants is associated with asymmetric dimerization, Cancer Res. 73 (22) (2013) 6770–6779.
[17] C.C. Valley, D.J. Arndt-Jovin, N. Karedla, M.P. Steinkamp, A.I. Chizhik, W. S. Hlavacek, B.S. Wilson, K.A. Lidke, D.S. Lidke, Enhanced dimerization drives ligand-independent activity of mutant epidermal growth factor receptor in lung cancer, Mol. Biol. Cell 26 (22) (2015) 4087–4099.
[18] K. Ota, T. Harada, K. Otsubo, A. Fujii, Y. Tsuchiya, K. Tanaka, I. Okamoto, Y. Nakanishi, Visualization and quantitation of epidermal growth factor receptor homodimerization and activation with a proximity ligation assay, Oncotarget 8 (42) (2017) 72127–72132.
[19] H. Yagi, M. Yagi-Utsumi, R. Honda, Y. Ohta, T. Saito, M. Nishio, S. Ninagawa, K. Suzuki, T. Anzai, Y. Kamiya, K. Aoki, M. Nakanishi, T. Satoh, K. Kato, Improved secretion of glycoproteins using an N-glycan-restricted passport sequence tag recognized by cargo receptor, Nat. Commun. 11 (1) (2020) 1368.
[20] K. Yamana, J. Inoue, R. Yoshida, J. Sakata, H. Nakashima, H. Arita, S. Kawaguchi, S. Gohara, Y. Nagao, H. Takeshita, M. Maeshiro, R. Liu, Y. Matsuoka, M. Hirayama, K. Kawahara, M. Nagata, A. Hirosue, R. Toya, R. Murakami, Y. Kuwahara, M. Fukumoto, H. Nakayama, Extracellular vesicles derived from radioresistant oral squamous cell carcinoma cells contribute to the acquisition of radioresistance via the miR-503-3p-BAK axis, J Extracell Vesicles 10 (14) (2021) e12169.
[21] R. Liu, K. Ota, E. Iwama, Y. Yoneshima, K. Tanaka, H. Inoue, T. Tagawa, Y. Oda, M. Mori, Y. Nakanishi, I. Okamoto, Quantification of HER family dimers by proximity ligation assay and its clinical evaluation in non-small cell lung cancer patients treated with osimertinib, Lung Cancer (2021).
[22] J. Baulida, M.H. Kraus, M. Alimandi, P.P. Di Fiore, G. Carpenter, All ErbB receptors other than the epidermal growth factor receptor are endocytosis impaired, J. Biol. Chem. 271 (9) (1996) 5251–5257.
[23] K.E. Longva, F.D. Blystad, E. Stang, A.M. Larsen, L.E. Johannessen, I.H. Madshus, Ubiquitination and proteasomal activity is required for transport of the EGF receptor to inner membranes of multivesicular bodies, J. Cell Biol. 156 (5) (2002) 843–854.
[24] M. Pietila, P. Sahgal, E. Peuhu, N.Z. Jantti, I. Paatero, E. Narva, H. Al-Akhrass, J. Lilja, M. Georgiadou, O.M. Andersen, A. Padzik, H. Sihto, H. Joensuu, M. Blomqvist, I. Saarinen, P.J. Bostrom, P. Taimen, J. Ivaska, SORLA regulates endosomal trafficking and oncogenic fitness of HER2, Nat. Commun. 10 (1) (2019) 2340.
[25] E.E. Er, M.C. Mendoza, A.M. Mackey, L.E. Rameh, J. Blenis, AKT facilitates EGFR trafficking and degradation by phosphorylating and activating PIKfyve, Sci. Signal. 6 (279) (2013) ra45.
[26] G.D. Lewis Phillips, G. Li, D.L. Dugger, L.M. Crocker, K.L. Parsons, E. Mai, W. A. Blattler, J.M. Lambert, R.V. Chari, R.J. Lutz, W.L. Wong, F.S. Jacobson, H. Koeppen, R.H. Schwall, S.R. Kenkare-Mitra, S.D. Spencer, M.X. Sliwkowski, Targeting HER2-positive breast cancer with trastuzumab-DM1, an antibody-cytotoxic drug conjugate, Cancer Res. 68 (22) (2008) 9280–9290.
[27] H.K. Erickson, P.U. Park, W.C. Widdison, Y.V. Kovtun, L.M. Garrett, K. Hoffman, R. J. Lutz, V.S. Goldmacher, W.A. Blattler, Antibody-maytansinoid conjugates are activated in targeted cancer cells by lysosomal degradation and linker-dependent intracellular processing, Cancer Res. 66 (8) (2006) 4426–4433.
[28] S.R. Shinde, S. Maddika, PTEN modulates EGFR late endocytic trafficking and degradation by dephosphorylating Rab7, Nat. Commun. 7 (2016) 10689.
[29] D. Westover, J. Zugazagoitia, B.C. Cho, C.M. Lovly, L. Paz-Ares, Mechanisms of acquired resistance to first- and second-generation EGFR tyrosine kinase inhibitors, Ann. Oncol. 29 (suppl_1) (2018) i10–i19.
[30] J.C. Soria, Y. Ohe, J. Vansteenkiste, T. Reungwetwattana, B. Chewaskulyong, K. H. Lee, A. Dechaphunkul, F. Imamura, N. Nogami, T. Kurata, I. Okamoto, C. Zhou, B.C. Cho, Y. Cheng, E.K. Cho, P.J. Voon, D. Planchard, W.C. Su, J.E. Gray, S.M. Lee,

R. Hodge, M. Marotti, Y. Rukazenkov, S.S. Ramalingam, F. Investigators, Osimertinib in Untreated EGFR-Mutated Advanced Non-Small-Cell Lung Cancer, N. Engl. J. Med. 378 (2) (2018) 113–125.
[31] M. Jebbink, A.J. de Langen, M.C. Boelens, K. Monkhorst, E.F. Smit, The force of HER2 - A druggable target in NSCLC? Cancer Treat. Rev. 86 (2020), 101996.
[32] H.A. Yu, M.E. Arcila, N. Rekhtman, C.S. Sima, M.F. Zakowski, W. Pao, M.G. Kris, V. A. Miller, M. Ladanyi, G.J. Riely, Analysis of tumor specimens at the time of acquired resistance to EGFR-TKI therapy in 155 patients with EGFR-mutant lung cancers, Clin. Cancer Res. 19 (8) (2013) 2240–2247.
[33] D. Planchard, Y. Loriot, F. Andre, A. Gobert, N. Auger, L. Lacroix, J.C. Soria, EGFR-independent mechanisms of acquired resistance to AZD9291 in EGFR T790M-positive NSCLC patients, Ann. Oncol. 26 (10) (2015) 2073–2078.
[34] K. Yonesaka, N. Takegawa, S. Watanabe, K. Haratani, H. Kawakami, K. Sakai, Y. Chiba, N. Maeda, T. Kagari, K. Hirotani, K. Nishio, K. Nakagawa, An HER3-targeting antibody-drug conjugate incorporating a DNA topoisomerase I inhibitor U3–1402 conquers EGFR tyrosine kinase inhibitor-resistant NSCLC, Oncogene 38 (9) (2019) 1398–1409.
[35] S. La Monica, D. Cretella, M. Bonelli, C. Fumarola, A. Cavazzoni, G. Digiacomo, L. Flammini, E. Barocelli, R. Minari, N. Naldi, P.G. Petronini, M. Tiseo, R. Alfieri, Trastuzumab emtansine delays and overcomes resistance to the third-generation EGFR-TKI osimertinib in NSCLC EGFR mutated cell lines, J. Exp. Clin. Cancer Res. 36 (1) (2017) 174.
[36] D. Cretella, F. Saccani, F. Quaini, C. Frati, C. Lagrasta, M. Bonelli, C. Caffarra, A. Cavazzoni, C. Fumarola, M. Galetti, S. La Monica, L. Ampollini, M. Tiseo, A. Ardizzoni, P.G. Petronini, R.R. Alfieri, Trastuzumab emtansine is active on HER-2 overexpressing NSCLC cell lines and overcomes gefitinib resistance, Mol. Cancer 13 (2014) 143.
[37] P.A. Janne, C. Baik, W.C. Su, M.L. Johnson, H. Hayashi, M. Nishio, D.W. Kim, M. Koczywas, K.A. Gold, C.E. Steuer, H. Murakami, J.C. Yang, S.W. Kim, M. Vigliotti, R. Shi, Z. Qi, Y. Qiu, L. Zhao, D. Sternberg, C. Yu, H.A. Yu, Efficacy and Safety of Patritumab Deruxtecan (HER3-DXd) in EGFR Inhibitor-Resistant, EGFR-Mutated Non-Small Cell Lung Cancer, Cancer Discov. 12 (1) (2022) 74–89.
[38] G.D. Lewis, I. Figari, B. Fendly, W.L. Wong, P. Carter, C. Gorman, H.M. Shepard, Differential responses of human tumor cell lines to anti-p185HER2 monoclonal antibodies, Cancer Immunol. Immunother. 37 (4) (1993) 255–263.